Available online at www.sciencedirect.com
ScienceDirect
Journal of Catalysis 243 (2006) 14–24
JOURNAL OF CATALYSIS
www.elsevier.com/locate/jcat

Influence of molar ratio on Pd–Pt catalysts for methane combustion

K. Persson [a,*], A. Ersson [a], K. Jansson [b], J.L.G. Fierro [c], S.G. Järås [a]

[a] *Department of Chemical Engineering and Technology, KTH Chemical Technology, Teknikringen 42, SE-100 44, Stockholm, Sweden*
[b] *Arrhenius Laboratory, Department of Inorganic Chemistry, University of Stockholm, S. Arrhenius väg 12, SE-106 91, Stockholm, Sweden*
[c] *ICP—Instituto de Catálisis y Petroleoquímica, CSIC, Cantoblanco, Madrid ES-28049, Spain*

Received 26 April 2006; revised 22 June 2006; accepted 22 June 2006

Available online 8 August 2006

Abstract

The catalytic oxidation of methane was investigated over six catalysts with different palladium and platinum molar ratios. The catalysts were characterised by TEM, EDS, XPS, PXRD and temperature-programmed oxidation. The results suggest that in the bimetallic catalysts, an alloy between Pd and Pt was formed in close contact with the PdO phase, with an exception for the Pt-rich catalyst, where no PdO was observed. It was found that the molar ratio between palladium and platinum clearly influences both the activity and the stability of methane conversion. By adding small amounts of platinum into the palladium catalyst, improved activity was obtained in comparison with the monometallic palladium catalyst. However, higher amounts of platinum are required for stabilising the methane conversion. The most promising catalysts with respect to both activity and stability were $Pd_{67}Pt_{33}$ and $Pd_{50}Pt_{50}$. The platinum-rich catalyst showed very poor activity for methane conversion.

Keywords: Palladium; Platinum; Bimetal; Methane; Catalytic oxidation; TEM; XRD; TPO; XPS; Stability

1. Introduction

Catalytic combustion is a promising technique for reducing thermal NO_x from gas turbine combustors [1]. One of the more common fuels used in these systems is natural gas, which is a relatively clean fuel with a high hydrogen to carbon ratio, hence producing less of the greenhouse gas CO_2; it is also available worldwide. The main combustible component of natural gas is methane. Because supported palladium catalysts have an excellent activity for complete oxidation of methane, they are often proposed for catalysts in gas turbine combustors [2,3]. But palladium-supported catalysts have some weaknesses. One important issue is the poor stability of methane conversion at steady-state operation [4–8]. Most researchers agree that the most active form of palladium is palladium oxide, PdO. However, it has been found that the initially high activity drops significantly during operation, resulting in an increasing difficulty in igniting the fuel. This could be due in part to the transformation of PdO into metallic palladium. This decomposition appears at around 750 °C during heating. During cooling, the reoxidation take place at a lower temperature than the decomposition, creating a hysteresis [9,10]. This may cause fluctuations during combustion. The PdO decomposition may explain some, but not all, of the instability experienced during methane combustion over palladium catalysts. Formation of less active palladium hydroxides and the occurrence of different types of palladium oxides may be other explanations. Clearly, pure palladium catalysts cannot meet the demands for stable conversion that will be placed on a commercial application.

It has been suggested that the performance of supported palladium catalysts may be improved by adding certain metals. Most reports consider methane oxidation over Pd–Pt catalysts. The addition of platinum to a palladium catalyst has been shown to stabilise the activity for methane oxidation in comparison with monometallic palladium catalysts [4–7,11]. The stability of the methane conversion makes this type of catalysts more attractive than the monometallic palladium catalyst. The addition of platinum to the palladium catalysts is also effective in preventing particle growth, resulting in less sintering [4,12].

* Corresponding author. Fax: +46 8 108579.
E-mail address: katarina.persson@ket.kth.se (K. Persson).

0021-9517/$ – see front matter
doi:10.1016/j.jcat.2006.06.019

Opinion is divided regarding the effect on the level of methane oxidation when platinum is added to the palladium catalysts. A considerable portion of the papers reach a positive conclusion [4,11,13,14]. However, it has also been reported that the initial activity is lower for the bimetallic Pd–Pt catalysts than for the monometallic palladium catalysts [7,12]. An explanation for the diverse results might be the different molar ratios for palladium and platinum used in the experiments.

The purpose of this study was to investigate the catalytic oxidation of methane over a range of palladium and platinum catalysts with different molar ratios. Activity and the ability to maintain stable methane conversion were evaluated for the various catalysts. Characterisation techniques, such as TEM, EDS, XPS, PXRD, BET, and TPO, have been used to determine the changes in morphology, element distribution, and redox properties when the platinum content is increased in the palladium catalyst.

2. Experimental

2.1. Catalyst preparation

Catalysts comprising palladium and platinum at various molar ratios were prepared for this study; the details regarding these catalysts are summarised in Table 1. All catalysts had a loading of 470 μmol metal/g catalyst powder, equal to the amount of metal in the 5 wt% Pd on alumina catalyst. The amounts of metals in the catalysts were confirmed by ICP analyses. All catalysts were supported on γ-Al_2O_3 (PURALOX HP-14/150, Sasol Germany GmbH).

The alumina powder was impregnated with the metal/metals by the incipient wetness technique. The bimetallic catalysts were accomplished by co-impregnation of the two metals by mixing solutions of palladium and platinum nitrate. The metal solution was dripped onto the alumina and carefully mixed. This procedure was repeated twice, with a drying step at 300 °C for 4 h in between. The resulting samples were then calcined at 1000 °C for 1 h.

The catalyst powders were mixed with ethanol, and the resulting slurries were ball-milled for 24 h. Cordierite monoliths (400 cpsi, Corning), with ϕ 14 mm and length 10 mm, were dip-coated with the slurry, followed by a drying step at 100 °C. This procedure was repeated until 20 wt% of catalyst material was fixed on the monolith. The coated monolith was then calcined at 1000 °C for 2 h.

2.2. Characterisation

The surface areas of all catalyst powders were measured by nitrogen adsorption at liquid N_2 temperature in a Micromeritics ASAP 2010 instrument. The surface area was determined according to the Brunauer–Emmett–Teller (BET) theory. The samples were degassed in vacuum for at least 2 h at 250 °C before analysis.

The CO-chemisorption measurements were performed on the catalyst powder using a volumetric technique. Before the measurements, the samples were dried in vacuum at 120 °C, reduced in a flow of H_2 at 300 °C for 1 h, evacuated at 300 °C for 1 h, and then cooled to 35 °C. The CO chemisorption analyses were then carried out using a dual-isotherm method.

Inductively coupled plasma–atomic emission spectroscopy (ICP-AES) was performed on all catalyst powders to verify the amounts of noble metals. The crystalline phases in the various catalysts were monitored by powder X-ray diffraction (PXRD), using a diffractometer (Siemens Diffraktometer D5000) and a Guinier–Hägg camera with a radius of 40 mm. In the latter case, Si was added as an internal standard, and the powder X-ray photographs were evaluated by the Scanner System program package [15] to obtain the d-values. Using the JCPD database, the phases were identified and unit cell parameters were calculated for each phase. Using the diffractometer data, mean crystallite size estimation was made using the fundamental parameters approach application of the *TOPAS v2.0* software.

The redox properties of the various catalysts were analysed by temperature-programmed oxidation (TPO). The analyses were carried out using a Micromeritics AutoChem 2910, equipped with a thermal conductivity detector. A continuous flow of 5 vol% O_2/He was passed over 100 mg of calcined catalyst powder. The temperature was increased from 300 to 900 °C at a rate of 10 °C/min, followed by a decrease down to 300 °C. The temperature cycle was repeated twice; the results from the second cycle are presented in this paper.

The morphology and size of the noble metal particles on the alumina washcoat were studied by transmission electron microscopy (TEM) using a JEOL 2000 FX microscope equipped with an energy-dispersive X-ray spectroscopy (EDXS) detector (LINK AN 10000).

Surface analyses of the samples were performed using a VG Escalab 200R electron spectrometer equipped with a hemispherical electron analyser and an Al$K\alpha$ ($h\nu = 1486.6$ eV; 1 eV $= 1.6302 \times 10^{-19}$ J) 120-W X-ray source. The pow-

Table 1
The nomenclature, the metal loading, the BET surface area, CO uptake and the crystallite size of the different catalysts

Sample	Composition	Pd loading (wt%)	Pt loading (wt%)	BET surface area (m^2/g)	CO uptake (μmol/g catalyst)	Crystallite size[a] PdO (nm)	Crystallite size[a] Pd–Pt (nm)
$Pd_{100}Pt_0$	1:0 Pd//Al_2O_3	5.1	0	102	7.3	27	–
$Pd_{80}Pt_{20}$	4:1 Pd:Pt//Al_2O_3	4.1	1.8	111	10.7	21	27
$Pd_{67}Pt_{33}$	2:1 Pd:Pt//Al_2O_3	3.0	3.3	91	5.2	22	47
$Pd_{50}Pt_{50}$	1:1 Pd:Pt//Al_2O_3	2.6	4.7	107	7.0	23	36
$Pd_{33}Pt_{67}$	1:2 Pd:Pt//Al_2O_3	1.5	5.5	95	3.1	–	73
Pd_0Pt_{100}	0:1 Pt//Al_2O_3	0	8.2	109	8.6	–	27

[a] Estimated by TOPAS—Fundamental Parameter Approach.

der samples were pressed into 8-mm-diameter stainless steel troughs, mounted on a sample rod. The unit was placed in the pretreatment chamber and degassed for 1 h at ambient temperature before being transferred to the analysis chamber. The base pressure in the analysis chamber was maintained below 4×10^{-9} mbar during data acquisition. The pass energy of the analyser was set to 50 eV, for which the resolution, as measured by the full width at half maximum (FWHM) of the $Au4f_{7/2}$ core level, was 1.7 eV. The binding energies were referenced to the Al2p peak of the alumina support at 74.5 eV. Data processing was performed with the *XPS peak* program. The spectra were decomposed using the least squares fitting routine by a Gaussian/Lorentzian (90/10) product function provided with the software. After subtracting a Shirley background, the atomic fractions were calculated using peak areas normalised on the basis of sensitivity factors provided by the manufacturer.

2.3. Activity tests

The catalytic activity for methane oxidation over the various catalysts was tested in a conventional tubular reactor, working at atmospheric pressure. A gas mixture of 1.5 vol% CH_4 in air was fed to the reactor at a space velocity of 250,000 h^{-1}. The temperature was recorded by a thermocouple placed upstream of the monolith. The composition of the product gas was analysed by an on-line gas chromatograph (GC Varian 3800) equipped with a thermal conductivity detector. Two different activity tests—a transient test and a steady-state test—were performed for each catalyst. For the transient tests, the temperature was varied continuously at a rate of 5 °C/min. Two consecutive heating and cooling cycles at temperatures from 300 to 900 °C were conducted; the results from the second cycle are used in this study. For the steady-state tests, the experiments were initiated at 435 °C and the temperature was increased stepwise up to 750 °C. The operation parameters were held constant for 1 h at each temperature.

3. Results

3.1. BET surface area and CO chemisorption

The specific BET surface areas of the catalysts after calcination at 1000 °C are compiled in Table 1. Because all catalysts were supported on the same support material (i.e., alumina), the BET surface areas should have been similar. However, the BET surface area varied between 111 and 91 m^2/g. No specific trend could be correlated to the noble metals deposited on the alumina.

The CO-chemisorption measurements are also presented in Table 1. $Pd_{80}Pt_{20}$, which had the highest BET surface area, also achieved the highest CO uptake, 10.7 μmol/g of catalyst. The monometallic platinum catalyst, Pd_0Pt_{100}, had a CO uptake of 8.6 of μmol/g catalyst, slightly higher than that for the monometallic palladium catalyst, $Pd_{100}Pt_0$, at 7.3 μmol/g of catalyst. Even though $Pd_{50}Pt_{50}$ had a slightly higher surface area than the monometallic Pd catalyst, it had a lower CO uptake, 7.0 μmol/g of catalyst. $Pd_{67}Pt_{33}$, which had the lowest BET surface area of the samples, had a CO uptake of 5.2 μmol/g of catalyst. The catalyst with the lowest CO uptake was $Pd_{67}Pt_{33}$, with 3.1 μmol/g of catalyst. The CO uptake reflects the dispersion of the noble metals. However, because the adsorption geometry of CO is not known for the Pd–Pt bimetals, calculating an exact value of the dispersion is difficult.

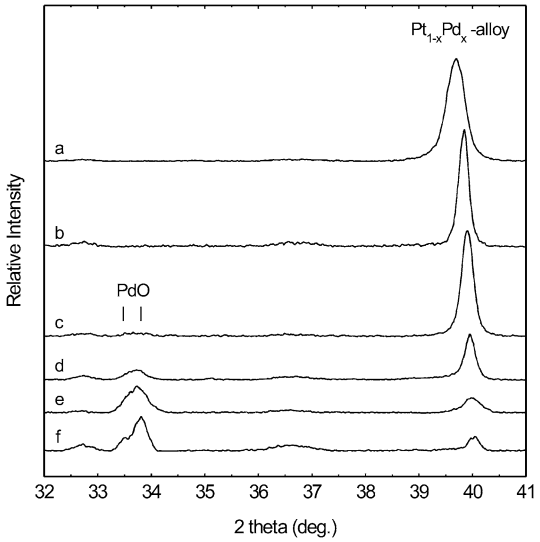

Fig. 1. PXRD patterns of as-prepared (a) Pd_0Pt_{100}, (b) $Pd_{33}Pt_{67}$, (c) $Pd_{50}Pt_{50}$, (d) $Pd_{67}Pt_{33}$, (e) $Pd_{80}Pt_{20}$ and (f) $Pd_{100}Pt_0$.

3.2. PXRD

θ-Al_2O_3 was observed in the PXRD patterns for all as-prepared catalysts. The Pd_0Pt_{100} catalyst exhibited only metallic platinum, whereas the pure Pd catalyst exhibited mainly PdO and minor amounts of metallic palladium. For all bimetallic catalysts, a $Pt_{1-x}Pd_x$ alloy was found; for the bimetallic catalysts with >50 at% Pd, PdO was observed together with the alloy (see Fig. 1). The alloy composition varied with the catalyst nominal composition, and using Vegard's law for solid solutions, it was calculated to be in the range of $0.33 < x < 0.55$; see also Fig. 7.

The results from estimation of the mean crystallite sizes are given in Table 1. The PdO crystallites were found to be in the range of 21–27 nm, whereas a wider variation was found for the alloy crystallites, with a range of 27–73 nm. The pure Pt catalyst exhibited a mean size of 27 nm.

3.3. TPO

The results from the TPO analyses are shown in Fig. 2. The TPO profile of monometallic palladium catalyst, $Pd_{100}Pt_0$, displayed three positive peaks at 760, 820 and 875 °C. These peaks are located close to one another; their onset temperature is 730 °C, and they end first at 900 °C. These peaks arise from the oxygen release occurring when different forms of PdO decompose [16]. During cooling, only one negative peak was detected, initiating at 620 °C. It is generally agreed that this peak represents Pd reoxidation. The difference between the onset temperatures of the decomposition and the reoxidation resulted in a

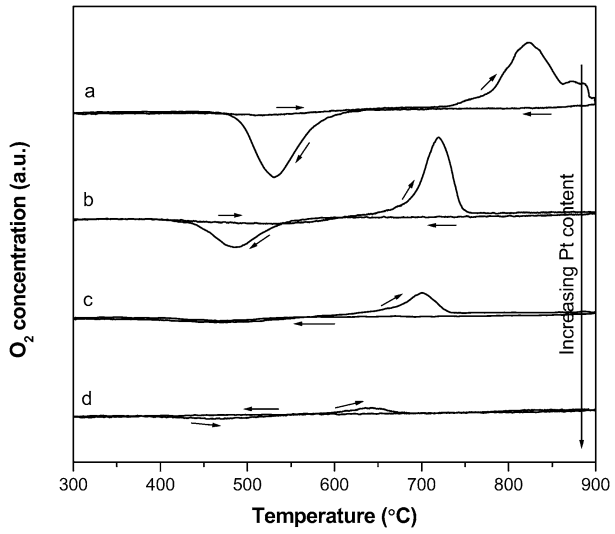

Fig. 2. Temperature-programmed oxidation plots of the palladium-rich catalysts (a) $Pd_{100}Pt_0$, (b) $Pd_{80}Pt_{20}$, (c) $Pd_{67}Pt_{33}$ and (d) $Pd_{50}Pt_{50}$.

hysteresis of 110 °C, as is typical for supported palladium catalysts.

When a part of the palladium was substituted by platinum, only a single positive peak was observed during heating. The peak was shifted toward lower onset temperature with increasing Pt content. The peak intensity also decreased with increasing platinum content, indicating that less oxygen was released from the catalysts. $Pd_{80}Pt_{20}$ had the strongest reduction peak of the bimetallic catalysts; the reduction started at 650 °C and ended at 760 °C. The reduction of $Pd_{67}Pt_{33}$ started at 630 °C and ended at 740 °C. $Pd_{50}Pt_{50}$ had a very small peak starting at 595 °C and ending at 690 °C. For the catalysts with more platinum than palladium (i.e., $Pd_{33}Pt_{67}$ and Pd_0Pt_{100}), no peaks were detected in the temperature range used in the TPO analyses.

Common to all samples that demonstrated a response in the TPO analysis was slow reoxidation that continued during heating. This can be seen in the TPO profiles as a broad negative peak before the reduction peak. This phenomenon was also seen for the monometallic palladium catalyst.

During cooling, $Pd_{80}Pt_{20}$ initiated reoxidation at 550 °C, resulting in a temperature hysteresis of only 100 °C. $Pd_{67}Pt_{33}$ began to reoxidise at 545 °C, resulting in a temperature hysteresis of 85 °C. For $Pd_{50}Pt_{50}$, no reoxidation was observed during cooling, but a negative peak was seen during heating, indicating that reoxidation was more difficult but hysteresis was lower with increasing Pt content.

3.4. TEM

TEM images of the six different catalysts are shown in Figs. 3a–3f. According to the elemental analyses, the alumina support appears as grayish, elongated, partly transparent particles. In the support material, dark dots represent the noble metals, according to the elementary analyses. In all catalysts, the noble metal particles were well distributed in the alumina support. The sizes of the noble metal particles were determined from numerous investigated fragments. All catalysts had metal particle sizes of 30–80 nm, except for $Pd_{33}Pt_{67}$ m, which exhibited a very wide size variation of 20–200 nm.

A fragment of the catalyst material of $Pd_{100}Pt_0$ is shown in Fig. 3a. As can be seen, some of the Pd particles are facetted, indicating that they are single crystallites, whereas others seem to be agglomerates of smaller Pd-containing particles. Similar distributions of the particles were found in the bimetallic catalysts with more Pd than Pt.

Fig. 3b shows the sample of Pd_0Pt_{100}. The particles appear to be facetted and well distributed on the alumina surface. Fig. 3c shows two noble metal particles of the $Pd_{80}Pt_{20}$ sample. EDS measurements using a small electron spot size on both sides of the particles revealed that the greater part of the particles consisted of Pd, most likely as PdO. Both Pd and Pt were found in close contact with the PdO domain; this may be attributed to an alloy between Pd and Pt. This morphologic description of the particles is valued for the whole sample.

Fig. 3d shows a fragment of the catalyst material of $Pd_{67}Pt_{33}$. Again, an intimate contact between the indicated Pd–Pt alloy and PdO can be seen. Because the platinum content here is higher than that for $Pd_{80}Pt_{20}$, the alloy domain is considerably larger, almost half of the particle. Fig. 3e shows a representative image of $Pd_{50}Pt_{50}$. In this sample, the major part of the particle is the alloy between Pd and Pt, with only a small part containing PdO. When considering the $Pd_{33}Pt_{67}$ sample, the distribution of the particles is inconsistent, as shown in Fig. 3f. The particles vary in both size and composition.

To determine the element distribution in the bimetallic catalysts, EDS analyses were carried out by spot measurements on whole individual particles, including both the domains of PdO and Pd–Pt alloy. More than 60 different particles were analysed for each catalyst; the results are plotted in Figs. 4a–4d, with decreasing Pd content. The atomic percentages of Pd and Pt are given on the left y-axis; the molar ratio between Pd and Pt over the whole particles, on the right y-axis. Common to all catalysts is the absence of noble metals in the areas between the noble metal particles; only alumina was detected. For the palladium-rich catalysts and $Pd_{50}Pt_{50}$, the distribution between Pd and Pt was homogeneous between the particles; Pt was found only with Pd, and no individual Pt or Pd particles were found. However, in the $Pd_{33}Pt_{67}$ sample, the particles exhibited various particle compositions, ranging from pure platinum to a Pd:Pt ratio of 1:1. Palladium-containing particles without platinum were not found.

3.5. XPS

XPS measurements provide valuable information on the surface composition and oxidation state of the catalysts. The binding energies of Al2p, $Pd3d_{5/2}$, and $Pt4d_{5/2}$ of the catalysts are shown in Table 2. XPS spectra for $Pd3d_{5/2}$ on the catalysts containing palladium are displayed in Fig. 5. For the monometallic Pd catalyst, $Pd_{100}Pt_0$, only one component was found at a binding energy of 337.1 eV. This component was also observed in $Pd_{80}Pt_{20}$, but with a binding energy shifted slightly, to 337.3 eV. Considering the other bimetallic catalysts, two dif-

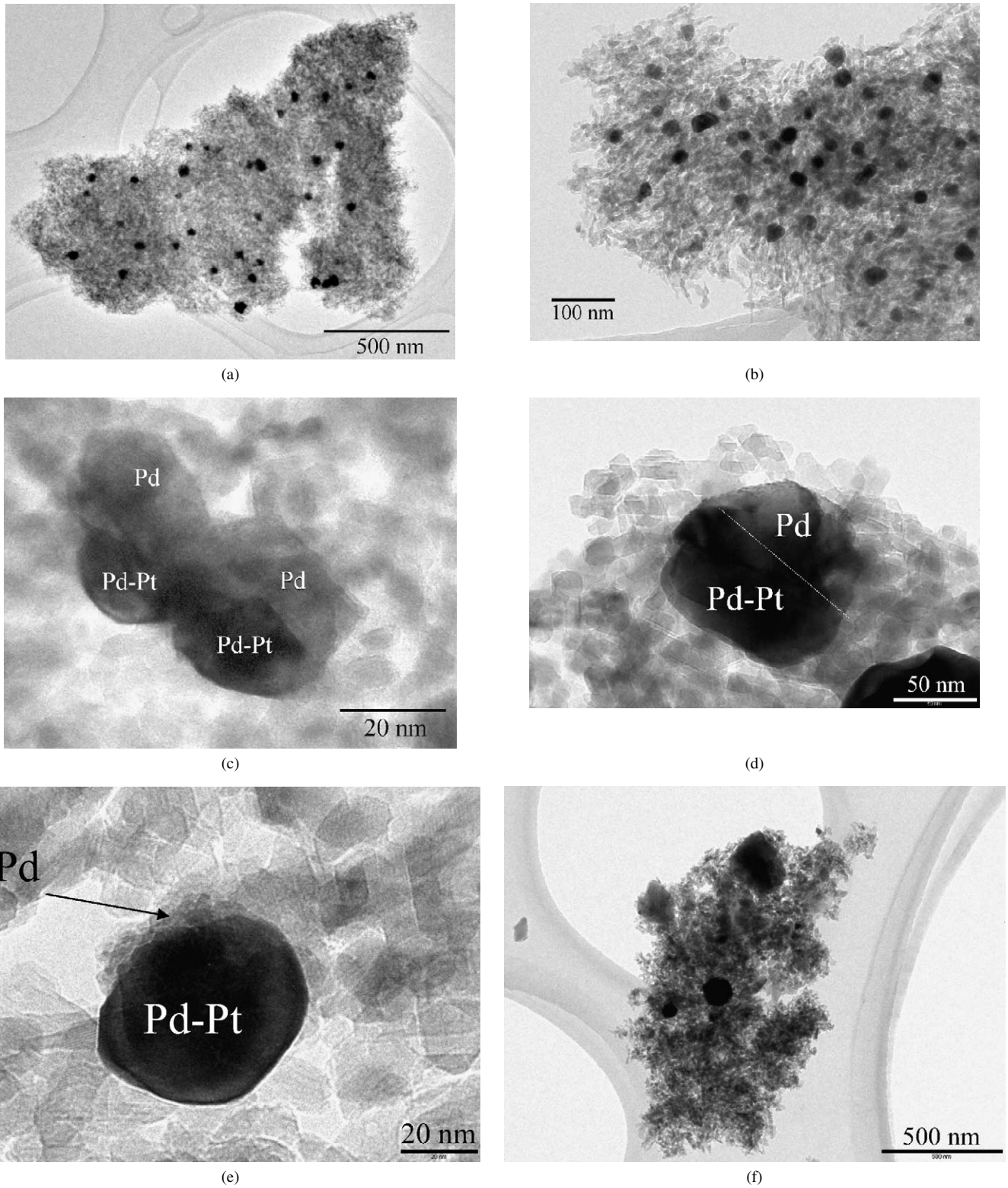

Fig. 3. TEM images of (a) $Pd_{100}Pt_0$, (b) Pd_0Pt_{100}, (c) $Pd_{80}Pt_{20}$, (d) $Pd_{67}Pt_{33}$, (e) $Pd_{50}Pt_{50}$, (f) $Pd_{33}Pt_{67}$.

ferent $Pd3d_{5/2}$ components were detected. The component at the higher binding energy is probably similar to that observed in the $Pd_{100}Pt_0$ and $Pd_{80}Pt_{20}$ samples. However, the binding energy increased with increasing platinum content, and $Pd_{33}Pt_{67}$ had a binding energy as high as 337.7 eV. According to the literature, a component at this high binding energy may be attributable to a higher oxidation state of palladium than Pd^{2+}, probably Pd^{4+} [17–19].

The second component had a binding energy of 336.0 eV, which may be associated with Pd^{2+} [17,19,20]. However, the value obtained in this study is at least 0.6–0.3 eV lower than the value presented in the literature. The value of this binding

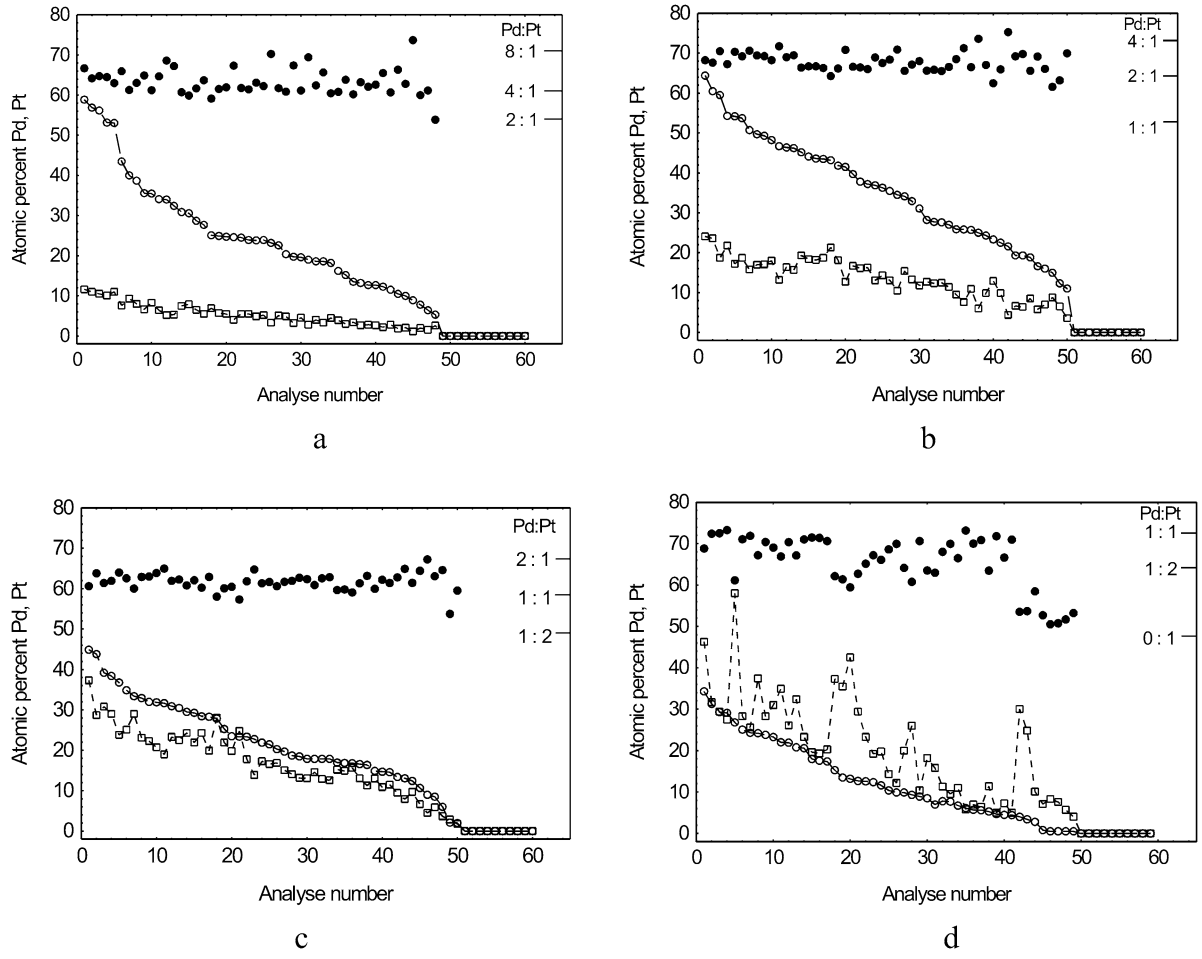

Fig. 4. Spot element analyses obtained by TEM/EDS on particles and Al_2O_3 material in the bimetallic catalysts for (a) $Pd_{80}Pt_{20}$, (b) $Pd_{67}Pt_{33}$, (c) $Pd_{50}Pt_{50}$, (d) $Pd_{33}Pt_{67}$. Pd, Pt and Pd:Pt ratio are represented by (○), (□) and (●), respectively.

Table 2
Binding energy of core electrons of the different catalysts

Catalyst	Al2p	Pd3d$_{5/2}$[a]	Pt4d$_{5/2}$[a]	O1s
$Pd_{100}Pt_0$	74.5	337.1	–	531.4
$Pd_{80}Pt_{20}$	74.5	337.3	314.4 (72) 316.8 (28)	531.5
$Pd_{67}Pt_{33}$	74.5	336.0 (22) 337.3 (78)	314.4 (78) 317.0 (22)	531.5
$Pd_{50}Pt_{50}$	74.5	336.0 (41) 337.5 (59)	314.5 (77) 317.1 (23)	531.5
$Pd_{33}Pt_{67}$	74.5	336.0 (65) 337.7 (35)	314.5 (82) 317.1 (18)	531.5
Pd_0Pt_{100}	74.4	–	314.5 (77) 317.1 (23)	531.5

[a] The numbers in parentheses are peak percentages.

energy was the same for the three catalysts. The ratio of the two different components varied with the platinum content in the sample, with $Pd_{67}Pt_{33}$ having 78% of the component at the higher binding energy but $Pd_{33}Pt_{67}$ having only 35%.

For platinum, only the Pt4d$_{5/2}$ was recorded, because the most intense Pt4f peak was overlapped by a very strong Al2p peak. The results are shown in Fig. 6 for all platinum-containing samples. Again, two components were observed; a major one at the lower binding energies (314.4–314.5 eV) associated with metallic platinum [21,22] and a minor one at higher binding energies (316.8–317.1 eV) signifying the presence of oxidised platinum species, probably as PtO_2 [21,23]. The binding energies of the Pt^0 species were more or less constant for the monometallic and bimetallic samples. A slightly clearer shift was seen for the oxidised platinum species, with values of 316.8 eV for $Pd_{80}Pt_{20}$ and 317.1 eV for $Pd_{50}Pt_{50}$. No further changes were observed for the catalysts rich in platinum. Independent of the amount of palladium in the catalysts, only between 18 and 28% of the surface Pt was oxidised.

To study whether the Pd and Pt atoms are homogeneously distributed on the catalyst surface, the surface composition derived from XPS was plotted versus the nominal Pd composition, shown in Table 3 and Fig. 7. The data appear to reasonably fit a straight line, suggesting that both metals are uniformly distributed on the catalyst surface and none of the metal is segregated on the surface.

The same figure shows the solid solutions between Pd and Pt taken from PXRD and the total amounts of Pd and Pt in the samples obtained from ICP-AES. The total amounts of the metals appear to fit the theoretical values reasonably well, as shown by the dashed line. The values of the alloy composition are well below the nominal values at 0.8 and 0.67, but only slightly below the nominal values at 0.5. All of these values indicate that the

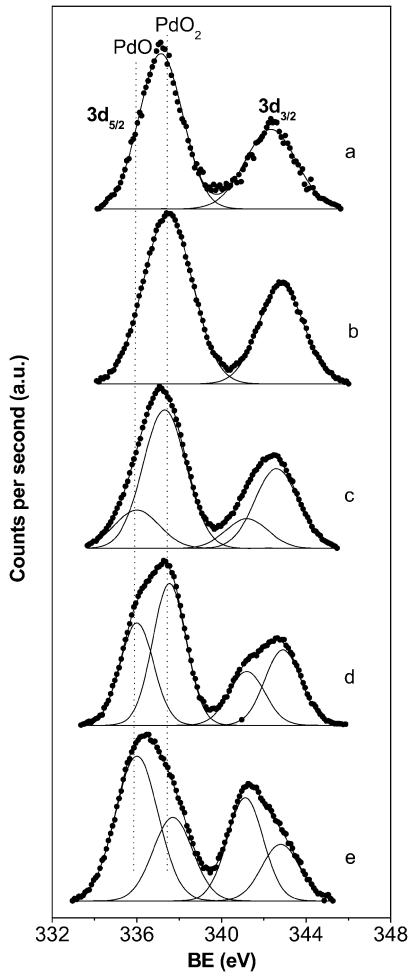

Fig. 5. Pd3d core level spectra of (a) $Pd_{100}Pt_0$, (b) $Pd_{80}Pt_{20}$, (c) $Pd_{67}Pt_{33}$, (d) $Pd_{50}Pt_{50}$ and (e) $Pd_{33}Pt_{67}$.

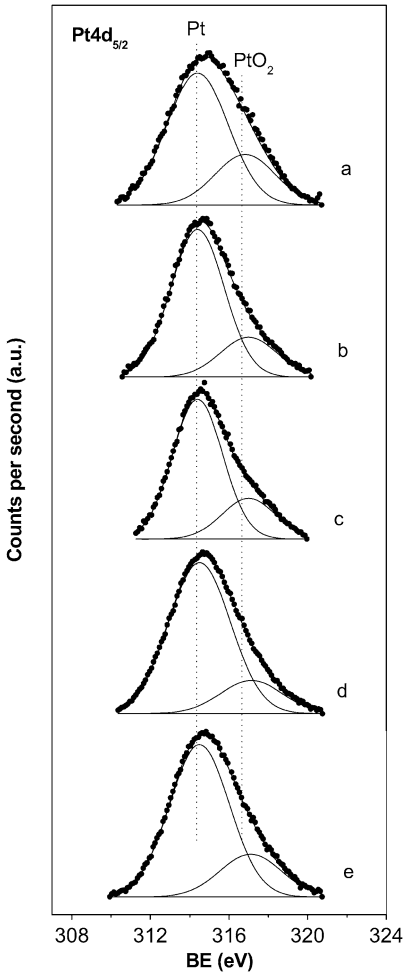

Fig. 6. $Pt4d_{5/2}$ core level spectra of (a) $Pd_{80}Pt_{20}$, (b) $Pd_{67}Pt_{33}$, (c) $Pd_{50}Pt_{50}$, (d) $Pd_{33}Pt_{67}$ and (e) Pd_0Pt_{100}.

alloys have compositions close to $Pt_{0.5}Pd_{0.5}$. At a nominal composition of 0.33, the experimental value was actually above the theoretical value, however, with an estimated error of ±0.02.

3.6. Transient activity tests

The results from the transient activity tests at heating and cooling are displayed in Figs. 8 and 9, respectively. Fig. 8 illustrates the combustion behaviour over the catalysts when the inlet gas was heated from 300 to 900 °C. $Pd_{100}Pt_0$ shows the typical behaviour for a monometallic palladium catalyst, with a drop in conversion occurring at 750 °C during heating. This drop has been attributed to the decomposition of PdO to metallic Pd, which is less active for methane combustion [10,24]. During the cooling, shown in Fig. 9, the metallic palladium began to reoxidise to PdO at 745 °C. With a further temperature decrease, methane conversion reached a local maximum at 540 °C.

Similar behaviour was observed for all bimetallic catalysts except $Pd_{33}Pt_{67}$. $Pd_{80}Pt_{20}$ had the highest activity of all bimetallic catalysts; it was even more active than the monometallic palladium catalyst at temperatures up to 540 °C. At higher temperatures, the activity was slightly lower than that for $Pd_{100}Pt_0$, and the drop in activity occurred at 690 °C. The recovery of activity occurred at 740 °C under cooling and followed the curve of $Pd_{100}Pt_0$, but with lower conversion. $Pd_{67}Pt_{33}$ had lower activity than $Pd_{80}Pt_{20}$, but the drop in activity was first observed at 730 °C. The reoxidation moved to 705 °C, however. $Pd_{50}Pt_{50}$ initially gave a lower conversion than $Pd_{67}Pt_{33}$, but at 570 °C its conversion exceeded that of $Pd_{67}Pt_{33}$. The drop in conversion appeared at 670 °C, and reoxidation was initiated at 650 °C.

$Pd_{33}Pt_{67}$ has a different combustion profile than the other bimetallic catalysts, with no drop in activity observed during heating. $Pd_{33}Pt_{67}$ had very poor activity up to 750 °C, after

Table 3
Surface atomic ratios between Pd and Pt

Catalyst	Pd/Al at	Pt/Al at	Pd/(Pd + Pt) theoretical	Pd/(Pd + Pt) experimental
$Pd_{100}Pt_0$	0.0066	–	1.00	1.00
$Pd_{80}Pt_{20}$	0.0029	0.0012	0.80	0.71
$Pd_{67}Pt_{33}$	0.0023	0.0011	0.67	0.68
$Pd_{50}Pt_{50}$	0.0015	0.0009	0.50	0.63
$Pd_{33}Pt_{67}$	0.0081	0.0136	0.33	0.37
Pd_0Pt_{100}	–	0.0046	0.00	0.00

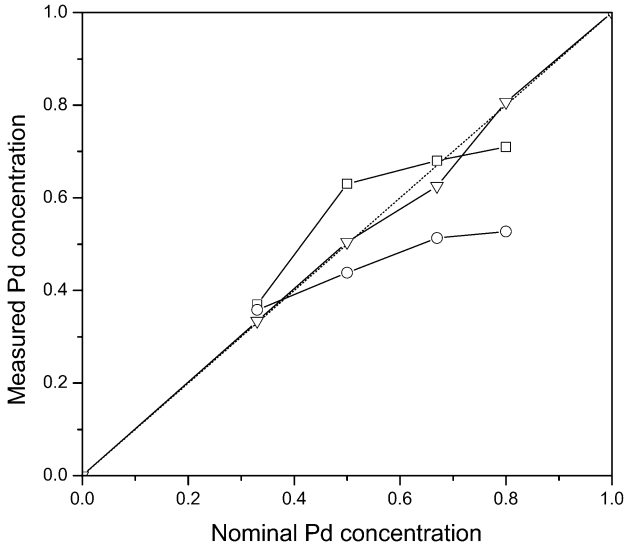

Fig. 7. Nominal composition versus surface (□), $Pt_{1-x}Pd_x$-alloy (○) and total composition (△), in as-prepared catalysts. The dashed line represents the theoretical value.

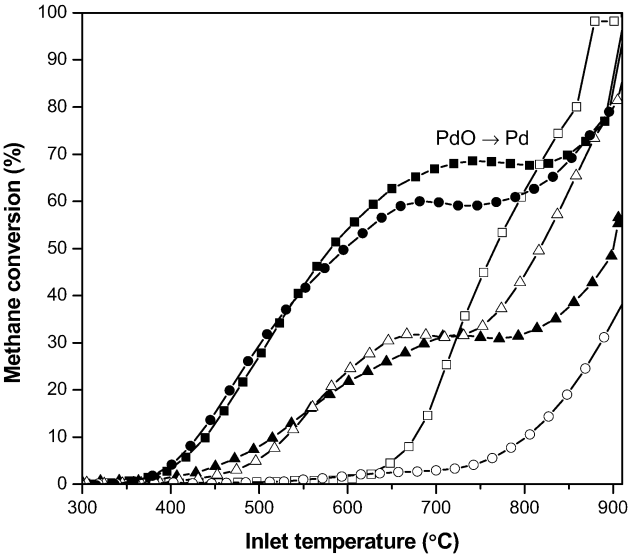

Fig. 8. Transient activity tests during heating. The methane conversion is shown versus the inlet temperature to the catalysts for $Pd_{100}Pt_0$ (■), $Pd_{80}Pt_{20}$ (●), $Pd_{67}Pt_{33}$ (▲), $Pd_{50}Pt_{50}$ (△), $Pd_{33}Pt_{67}$ (○) and Pd_0Pt_{100} (□).

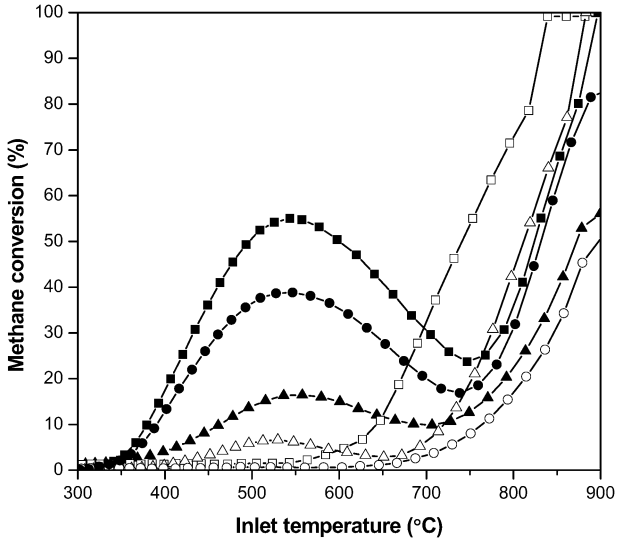

Fig. 9. Transient activity tests during cooling. The methane conversion is shown versus the inlet temperature to the catalysts for $Pd_{100}Pt_0$ (■), $Pd_{80}Pt_{20}$ (●), $Pd_{67}Pt_{33}$ (▲), $Pd_{50}Pt_{50}$ (△), $Pd_{33}Pt_{67}$ (○) and Pd_0Pt_{100} (□).

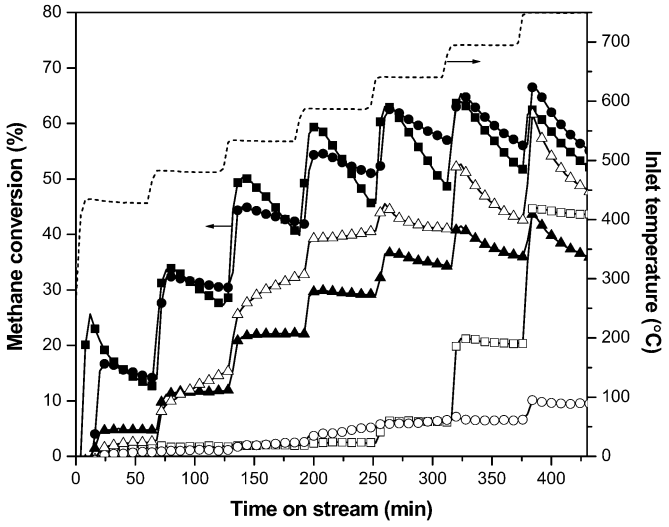

Fig. 10. Steady-state activity tests. Methane conversion as a function of time-on-stream for $Pd_{100}Pt_0$ (■), $Pd_{80}Pt_{20}$ (●), $Pd_{67}Pt_{33}$ (▲), $Pd_{50}Pt_{50}$ (△), $Pd_{33}Pt_{67}$ (○) and Pd_0Pt_{100} (□). The dotted line represents the temperature.

which methane conversion began to increase. Methane conversion never reached >50%, however. During cooling, the activity dropped quickly; below 645 °C, the catalyst had no activity. The monometallic Pt catalyst, Pd_0Pt_{100}, had a combustion profile similar to that of $Pd_{33}Pt_{67}$, but was much more active. The catalysts exhibited very low activity at temperatures below 630 °C, but greatly increased activity at higher temperatures. During cooling, the catalyst maintained its activity until 580 °C.

3.7. Steady-state activity tests

The results from the steady-state activity tests are shown in Fig. 10. A wide distribution of methane conversion among the various catalysts can be seen. $Pd_{100}Pt_0$ initially had the highest activity, but methane conversion decreased rapidly with time on stream. Methane conversion decreased for $Pd_{100}Pt_0$ even at temperatures as low as 435 °C, much lower than reported for PdO decomposition.

$Pd_{80}Pt_{20}$ initially gave excellent methane conversion, close to the values achieved for the monometallic palladium catalyst. However, the activity of $Pd_{80}Pt_{20}$ was unstable and, just as for the palladium-only catalyst, dropped with time on stream at all temperature steps. Nevertheless, the loss in conversion was not as great as that for the palladium-only catalyst; as a result, the $Pd_{80}Pt_{20}$ became more active at the end of each temperature step.

$Pd_{67}Pt_{33}$ and $Pd_{50}Pt_{50}$ were much more stable at temperatures below 640 °C. Above this temperature, methane conver-

sion decreased, probably due to PdO decomposition. $Pd_{50}Pt_{50}$ had a low activity for methane conversion for the first temperature step at 435 °C; for the subsequent steps, the activity actually increased with time on stream. $Pd_{67}Pt_{33}$ had a very stable methane conversion that neither decreased nor increased.

For the platinum-rich catalyst, $Pd_{33}Pt_{67}$, the conversion was low, although stable. Pd_0Pt_{100} had poor activity at the lower temperatures, but significant methane conversion at 695 °C.

4. Discussion

4.1. Catalyst materials

The results presented in this study suggest that the morphology varies with the Pd:Pt molar ratios. The monometallic catalysts, $Pd_{100}Pt_0$ and Pd_0Pt_{100}, have well-distributed particles of noble metals on the alumina surface, as shown by TEM. The XRD indicate that only one crystalline phase of platinum was present in the bulk of Pd_0Pt_{100} and that $Pd_{100}Pt_0$ consisted mostly of PdO.

When platinum is included in the palladium catalysts, an alloy is probably formed between the palladium and the platinum. This is indicated in the PXRD diffractograms as peaks in-between the 2 theta values corresponding to metallic Pd and Pt, respectively. Alloy formation is also supported by the element analyses, where Pt was found only in the presence of Pd. The composition of the alloy appears to be closer to $x = 0.5$ than the nominal value for the bimetallic catalysts with compositions containing >50 at% Pd, independent of the platinum content in the catalysts.

Even though an alloy was formed between the noble metals, the palladium-rich catalysts contained some PdO. Because the alloy had a composition close to $x = 0.5$, the remaining Pd in the catalyst formed PdO. Hence two domains, one containing the alloy and another containing PdO, coexisted in the particles of bimetallic catalysts. It is interesting that the two domains were always found in close contact with one another, except in the $Pd_{33}Pt_{67}$ catalyst, where individual Pt particles were found. Ongoing studies of used samples have shown that the indicated alloy in the bimetallic catalysts remains almost unaffected and still in close contact with the PdO phase after reaction.

According to TEM, $Pd_{33}Pt_{67}$ appears to have a very uneven structure, with particle sizes varying between 20 and 200 nm and irregular particle composition. No bulk PdO was observed in this catalyst; only different alloy formations and pure Pt particles were seen. The large particles are also indicated by the low CO uptake value.

From previous studies, it can be concluded that not all metals can form an alloy with palladium; the metal must be nobler than palladium [7]. Very few other metals can possibly form the same morphology as platinum and palladium, with divided particles. The results from the PXRD and TEM studies suggest that the fraction of the alloy in the catalysts increased with increasing the platinum content, at the same time as the PdO content decreased, probably because almost all of the Pt was alloyed with Pd.

The decreasing PdO content with increasing Pt is also in line with the TPO results. When the platinum content in the catalyst increased, the TPO peaks became smaller and shifted to lower temperatures. This observation is in agreement with the literature [5,7,25,26]. The TPO peak during heating most likely arose from PdO decomposition, as in the case of the monometallic Pd catalyst, with the size of the decomposition peak reflecting the amount of PdO in the sample. Hence, as the peak decreased with increasing Pt, less PdO was present in the sample. No peaks were observed for the Pt-rich catalysts; therefore, the palladium presumably was in a nonoxidised form in the Pt-rich catalysts. If the palladium occurred only in its metallic state, without alloying with Pt, then it would be oxidised to PdO. Hence, an alloy formation between Pd and Pt can be assumed.

Previous TPO studies in our lab have shown that the amount of PdO in the sample does not affect the onset temperature of the PdO decomposition, but affects only the intensity of the peaks [7]. Hence, the shift observed for the bimetallic catalysts in the TPO analyses is not due to the lower amounts of PdO, but does indicate promotion of PdO reduction by platinum.

The surface compositions were verified by XPS. It appears that the phases of the surface differed from those of the bulk, with higher oxidation states, palladium as Pd^{2+} and Pd^{4+}, and platinum as Pt^{4+}. Because both Pd components were in an oxidised state, the presumable alloy most likely was oxidised on the surface to some extent.

4.2. Activity and stability under conditions of methane conversion

The diverse results concerning the stability and level of methane conversion with varying platinum content suggest that the molar ratio significantly affects the catalytic properties. $Pd_{100}Pt_0$ initially had very high activity, but poor stability for methane conversion. The opposite was observed for Pd_0Pt_{100}, which exhibited very poor conversion at the lower temperatures and was active only above 630 °C. However, the platinum catalyst had stable conversion. Hence, combining the positive properties of respective catalysts would be preferable, as discussed below.

It has been suggested that adding platinum to the palladium catalysts increases the activity for methane combustion [4,11, 13,14], whereas others have reported lower activity when platinum is present [7,12]. In the present study, the $Pd_{80}Pt_{20}$ catalyst had higher activity at the lower temperatures of the transient test compared with the monometallic Pd catalyst. Conversely, the bimetallic catalysts with more platinum had lower activity than the $Pd_{100}Pt_0$ catalyst. This indicates that the amount of platinum added is crucial to the level of activity, which may explain the large variation of results reported in the literature. Other explanations for the widely varying results may be differences in the bases against which the catalysts are compared (e.g., based on a constant weight percentage of palladium with extra amounts of platinum, keeping the weight percentage of noble metals constant, etc.). In this study, the molar amounts of noble metals were kept constant, and the molar ratio between Pd and Pt was varied. Because monometallic palladium cata-

lysts have poor stability, the time at which the comparison is made is also important.

The TEM images of $Pd_{80}Pt_{20}$ indicate that small domains of alloy were located next to the PdO domains. In the case of monometallic Pd catalysts, it has been suggested that small amounts of metallic Pd on the PdO particles give enhanced activity compared with fully oxidised PdO particles [27,28]. Su et al. [29] explained this phenomenon by the effect of CH_4 adsorbed dissociatively on metallic Pd, with the formation of CH_x ($x = 3$–1) species and H atoms. The fragments of the methane molecules are then rapidly diffused to the Pd/PdO interface, where reduction of the oxide occurs. Hence, a good contact surface between the Pd and the PdO particles is important. Because the dissociation of the methane molecule has been suggested to be a very slow step in methane oxidation [30], an improvement in dissociation may result in improved activity. However, Carsten et al. [27] reported that sustaining the metallic phase of palladium under steady-state conditions in an oxidising atmosphere is difficult because the metallic particles are oxidised back to PdO. In our case with the bimetallic Pd–Pt catalysts, it appears that the metallic phase is maintained even in an oxidising atmosphere due to the alloy. Although the catalyst is calcined in air, the alloy is still present in the samples, as indicated by the PXRD studies. This may result in better activity compared with the monometallic Pd catalyst, despite the slightly lower PdO content in the $Pd_{80}Pt_{20}$ catalyst.

Another possible reason for the higher activity of $Pd_{80}Pt_{20}$ may be that the Pd–Pt alloy dissociatively adsorbs more oxygen molecules than the PdO phase, so that the alloy is providing the PdO with oxygen after reduction. Bedrane et al. [31] reported that metals were much more active than oxides in dissociated oxygen and that the Pt metal was better than the Pd metal. Therefore, it is possible that the alloy has superior properties for splitting the oxygen molecule, which may increase the activity.

Even though small amounts of metallic Pd–Pt appear to be beneficial for the activity of methane combustion, high amounts of metallic alloy cannot compensate for significantly lower PdO content in the catalyst. The $Pd_{67}Pt_{33}$ and $Pd_{50}Pt_{50}$ catalysts have considerably lower PdO content than the monometallic Pd catalysts. It is generally known that pure PdO catalysts are much more active than pure metallic palladium catalysts as well as Pt catalysts [24,32]. Therefore, it is not surprising that the $Pd_{67}Pt_{33}$ and $Pd_{50}Pt_{50}$ catalysts have lower activity, despite the high metallic fractions.

$Pd_{33}Pt_{67}$ has a very uneven structure with large particles and almost no PdO present in the catalyst. The alloy itself most likely has very poor activity for methane conversion. This is probably the explanation for the very poor activity, which was even lower than that of Pd_0Pt_{100}. The catalyst showed no PdO/Pd transformation during the transient activity tests, but had combustion behaviour similar to that of Pd_0Pt_{100}.

Not only the level of activity, but also the ability to maintain constant activity with time on stream, is affected by the molar ratio of palladium and platinum. Even though $Pd_{80}Pt_{20}$ showed excellent activity, it did not exhibit very good stability. Nevertheless, it achieved a better stability than the monometallic Pd catalyst, indicating that Pt hampered the activity loss, but the amount of Pt in $Pd_{80}Pt_{20}$ was not sufficient to stabilise the conversion. Increasing the amount of platinum in the catalysts improved the stability. $Pd_{67}Pt_{33}$ had a very stable conversion with time, even though the amount of PdO remained fairly high, most likely due to the close contact between the alloy and the PdO domains. It is interesting that the activity of the $Pd_{50}Pt_{50}$ catalyst increased with time. Previous studies at our laboratory indicate that the increase is due to slow formation of PdO during operation [33]. Because $Pd_{50}Pt_{50}$ has a low PdO content, which is needed for the oxidation step, an increased amount of PdO led to enhanced activity. $Pd_{67}Pt_{33}$ already has a fairly high amount of PdO, and an increase of PdO may not affect the activity so drastically.

The superior stability of the bimetallic Pd–Pt catalyst is in accordance with previous reports [4–7,11]. A possible reason for the improved stability is that Pt suppresses the particle growth of PdO [4]; however, this is probably not the only reason. Another possibility may be that Pt prevents water inhibition of the palladium catalysts. PdO is strongly inhibited by water, possibly due to formation of inactive $Pd(OH)_2$ on the surface [34,35]. It is difficult to avoid this type of deactivation, because water is one of the reaction products in methane combustion. Nomura et al. [11] reported that a bimetallic Pd–Pt catalyst was more stable than a monometallic Pd catalyst when water vapour was added to the feed stream. The higher water resistance of the Pd–Pt catalysts was attributed to a synergistic effect between Pd and Pt. Because the Pd_0Pt_{100} catalyst in this study had a stable conversion, water may have played a role in the decreased activity of $Pd_{100}Pt_0$.

In summary, the catalysts must contain sufficient PdO to be active at lower temperatures and sufficient Pd–Pt alloy to achieve a stable conversion. A good contact between the two types of domains also appears to be essential for both the stability and the level of activity.

5. Conclusion

To stabilise the activity over palladium catalyst during methane oxidation, a series of six different palladium and platinum catalysts with molar ratios ranging from pure palladium to pure platinum were tested. The results show that it is possible to stabilise the activity over the palladium catalyst by adding platinum in certain amounts. Our findings can be summarised as follows:

- The activity of the catalysts decreased in the following order for the transient activity tests during heating between 300 and 560 °C: $Pd_{80}Pt_{20} > Pd_{100}Pt_0 > Pd_{67}Pt_{33} > Pd_{50}Pt_{50} > Pd_0Pt_{100} > Pd_{33}Pt_{67}$.
- As shown by the transient activity tests, small amounts of Pt improved the catalytic activity of methane oxidation for monometallic Pd catalysts.
- Even though the activity was initially high, the catalysts may experience decreased activity with time. The stability for methane conversion was affected by the amount of Pt in the sample. Considering both the stability and the activ-

ity level for methane combustion, $Pd_{50}Pt_{50}$ and $Pd_{67}Pt_{33}$ are the most promising catalysts for methane combustion tested in this study.

- For all of the bimetallic Pd–Pt catalysts, an alloy between Pd and Pt was most likely in close contact with PdO, except for $Pd_{33}Pt_{67}$, in which no PdO was found.
- $Pd_{33}Pt_{67}$ had an unevenly distributed morphology with large particles and no PdO and very low activity, indicating that the $Pt_{1-x}Pd_x$ alloys with $x < 0.5$ had very poor activity.
- The more Pt content in the catalyst, the nobler it became (i.e., the less PdO content). Hence, the platinum-rich catalysts had very little PdO. Pt was not found alone, except in $Pd_{33}Pt_{67}$ and Pd_0Pt_{100}.
- The reoxidation of $Pd_{50}Pt_{50}$ was very slow, resulting in oxidation of the catalyst during the activity tests. Hence, the activity increased with time.

Acknowledgments

This work was supported by the Swedish Energy Agency. The authors thank Sasol Germany GmbH for providing the alumina support.

References

[1] W.C. Pfefferle, J. Energy 2 (1978) 142.
[2] E.M. Johansson, D. Papadias, P.O. Thevenin, A.G. Ersson, R. Gabrielsson, P.G. Menon, P.H. Björnbom, S.G. Järås, in: J.J. Spivey (Ed.), Catalysis—Specialists Periodical Reports, vol. 14, Royal Society of Chemistry, Cambridge, 1999, p. 183.
[3] D. Ciuparu, M.R. Lyubovsky, E. Altman, L.D. Pfefferle, A. Datye, Catal. Rev. 44 (2002) 593.
[4] K. Narui, H. Yata, K. Furuta, A. Nishida, Y. Kohtoku, T. Matsuzaki, Appl. Catal. A 179 (1999) 165.
[5] A. Ersson, H. Kušar, R. Carroni, T. Griffin, S. Järås, Catal. Today 83 (2003) 265.
[6] K. Persson, A. Ersson, A. Manrique Carrera, J. Jayasuriya, R. Fakhrai, T. Fransson, S. Järås, Catal. Today 100 (2005) 479.
[7] K. Persson, A. Ersson, K. Jansson, N. Iverlund, S. Järås, J. Catal. 231 (2005) 139.
[8] Y. Ozawa, Y. Tochihara, M. Nagai, S. Omi, Chem. Eng. Sci. 58 (2003) 671.
[9] R.J. Farrauto, M.C. Hobson, T. Kennelly, E.M. Waterman, Appl. Catal. A 81 (1992) 227.
[10] J.G. McCarty, Catal. Today 26 (1995) 283.
[11] K. Nomura, K. Noro, Y. Nakamura, Y. Yazawa, H. Yoshida, A. Satsuma, T. Hattori, Catal. Lett. 53 (1998) 167.
[12] R. Strobel, J.-D. Grunwaldt, A. Camenzind, S.E. Pratsinis, A. Baiker, Catal. Lett. 104 (2005) 9.
[13] H. Yamamoto, H. Uchida, Catal. Today 45 (1998) 147.
[14] C.L. Pieck, C.R. Vera, E.M. Peirotti, J.C. Yori, Appl. Catal. A 226 (2002) 281.
[15] K.E. Johansson, T. Palm, P.E. Werner, J. Phys. Sci. Instrum. 13 (1980) 1289.
[16] G. Groppi, C. Cristiani, L. Lietti, P. Forzatti, in: A. Corma, F.V. Melo, S. Mendioroz, J.L.G. Fierro (Eds.), Studies in Surface Science and Catalysis, vol. 130, Elsevier, Amsterdam, 2000, p. 3801.
[17] K.S. Kim, A.F. Grossman, N. Winograd, Anal. Chem. 46 (1974) 197.
[18] A.L. Guimaraes, L.C. Dieguez, M. Schmal, J. Phys. Chem. B 107 (2003) 4311.
[19] Y. Bi, G. Lu, Appl. Catal. B 41 (2003) 279.
[20] S.K. Ihm, Y.D. Jun, D.C. Kim, K.E. Jeong, Catal. Today 93–95 (2004) 149.
[21] J.Z. Shyu, K. Otto, Appl. Surf. Sci. 32 (1988) 246.
[22] B. Pawelec, R. Mariscal, R.M. Navarro, S. van Bokhorst, S. Rojas, J.L.G. Fierro, Appl. Catal. A 225 (2002) 223.
[23] V.K. Kaushik, Z. Phys. Chem. 173 (1991) 105.
[24] K. Sekizawa, M. Machida, K. Eguchi, H. Arai, J. Catal. 142 (1993) 655.
[25] W. Kuper, M. Blaauw, F. van der Berg, G. Graaf, Catal. Today 47 (1999) 377.
[26] N. Kraikul, S. Jitkarnka, A. Luengnaruemitchai, Appl. Catal. B 58 (2005) 143.
[27] J.N. Carstens, S.C. Su, A.T. Bell, J. Catal. 176 (1998) 136.
[28] J. Grunwaldt, M. Maciejewski, A. Baiker, Phys. Chem. Chem. Phys. 5 (2003) 1481.
[29] S.C. Su, J.N. Carstens, A.T. Bell, J. Catal. 176 (1998) 125.
[30] M. Aryafar, F. Zaera, Catal. Lett. 48 (1997) 173.
[31] S. Bedrane, C. Descorme, D. Duprez, Appl. Catal. A 289 (2005) 90.
[32] R. Prasad, L.A. Kennedy, E. Ruckenstein, Catal. Rev. Sci. Eng. 26 (1984) 1.
[33] K. Persson, A. Ersson, S. Colussi, A. Trovarelli, S.G. Järås, Appl. Catal. B 66 (2006) 175.
[34] C.F. Cullis, T.G. Nevell, D.L. Trimm, J. Chem. Soc. Faraday Trans. 68 (1972) 1406.
[35] R. Burch, P. Loader, F. Urbano, Catal. Today 27 (1996) 243.